Human Molecular Genetics, 2000, Vol. 9, No. 11 **1567–1574**

The neurofibromatosis 2 tumor suppressor protein interacts with hepatocyte growth factor-regulated tyrosine kinase substrate

Daniel R. Scoles[1], Duong P. Huynh[1], Mercy S. Chen[1], Stephen P. Burke[2], David H. Gutmann[2] and Stefan-M. Pulst[1,3,+]

[1]Neurogenetics Laboratory, CSMC Burns and Allen Research Institute, Cedars-Sinai Medical Center, School of Medicine, University of California at Los Angeles, 8700 Beverly Boulevard, Los Angeles, CA 90048, USA, [2]Department of Neurology, Washington University School of Medicine, Box 8111, 660 South Euclid Avenue, St Louis, MO 63110, USA and [3]Division of Neurology, Cedars-Sinai Medical Center, University of California at Los Angeles School of Medicine, 8631 West 3rd Street, 1145E, Los Angeles, CA 90048, USA

Received 2 February 2000; Revised and Accepted 3 May 2000 DDBJ/EMBL/GenBank accession no. AF260566

The neurofibromatosis 2 tumor suppressor protein schwannomin/merlin is commonly mutated in schwannomas and meningiomas. Schwannomin, a member of the 4.1 family of proteins, which are known to link the cytoskeleton to the plasma membrane, has little known function other than its ability to suppress tumor growth. Using yeast two-hybrid interaction cloning, we identified the HGF-regulated tyrosine kinase substrate (HRS) as a schwannomin interactor. We verified the interaction by both immunoprecipitation of endogenous HRS with endogenous schwannomin *in vivo* as well as by using bacterially purified HRS and schwannomin *in vitro*. We narrowed the regions of interaction to include schwannomin residues 256–579 and HRS residues from 480 to the end of either of two HRS isoforms. Schwannomin molecules with a L46R, L360P, L535P or Q538P missense mutation demonstrated reduced affinity for HRS binding. As HRS is associated with early endosomes and may mediate receptor translocation to the lysosome, we demonstrated that schwannomin and HRS co-localize at endosomes using the early endosome antigen 1 in STS26T Schwann cells by indirect immunofluorescence. The identification of schwannomin as a HRS interactor implicates schwannomin in HRS-mediated cell signaling.

INTRODUCTION

Mutations in the neurofibromatosis 2 (*NF2*) gene are found in the majority of benign nervous system tumors, including schwannomas, ependymomas and meningiomas. When inherited as a germline mutation, skin and ocular abnormalities are also seen (1). *NF2* gene mutations are found in nearly all sporadic vestibular schwannomas and half of sporadic meningiomas and ependymomas, suggesting that schwannomin is an important growth regulator for the derivative cells that give rise to these tumors (2–6).

The *NF2* gene product, schwannomin or merlin, has strong sequence homology with members of the 4.1 family of proteins that link the cytoskeleton to the plasma membrane, including ezrin, radixin and moesin (ERM proteins) (7,8). Co-localization of schwannomin with actin at the ruffling edge of the plasma membrane (lamellipodia) is consistent with this role (9,10). Schwannomin may act upstream of the small GTP-binding proteins Rho and Rac in human fibroblasts, which are known to regulate lamellipodial outgrowth in a variety of cell types (11). Schwannomin also has a perinuclear distribution and is localized in cytoplasmic punctata (12). ERM proteins interact with F-actin via their C-terminal ends. While the C-terminal half of schwannomin possesses the least homology with this region in the ERM proteins, schwannomin was recently demonstrated to possess an N-terminal actin-binding domain (13). Additionally, we demonstrated that the C-terminal half of schwannomin interacts with βII-spectrin, a strong F-actin-binding protein (14). Using *NF2* antisense DNA we showed that the actin cytoskeleton is reorganized upon removal of schwannomin from STS26T Schwann cells (14). This change in STS26T cells was associated with increased proliferation, altered morphology and loss of adhesion (15). In addition, we have shown that overexpression of schwannomin results in impairment of actin cytoskeletal-mediated functions, including cell spreading, attachment and motility (16).

Although bi-allelic loss of *NF2* in tumors and increased proliferation following down-regulation of *NF2* expression are consistent with schwannomin functioning as a tumor suppressor protein, the signal transduction pathway in which schwannomin exerts its suppressive effects has remained elusive. In addition, Schwann cell proliferation in general is poorly understood, in part due to the difficulties in culturing human Schwann cells. Hepatocyte growth factor (HGF) is a

[+]To whom correspondence should be addressed at: Division of Neurology, Cedars-Sinai Medical Center, Suite 1145E, 8631 West 3rd Street, Los Angeles, CA 90048, USA. Tel: +1 310 423 5166; Fax: +1 310 423 0149; Email: pulst@cshs.org

potent Schwann cell mitogen and motogen (17), but signaling cascades stimulated by HGF in Schwann cells have largely remained undefined. Identification of these pathways and the extracellular signals that schwannomin modulates are critical for understanding Schwann cell growth control.

We now report the identification of HGF-regulated tyrosine kinase substrate (HRS) as a protein that binds schwannomin. HRS has two main functional roles: (i) regulation of protein trafficking mediated by the endosome (18); (ii) binding to and inhibition of STAM, an activator of JAK/STAT signaling (19,20). Our study implicates schwannomin in HRS-mediated regulation of cell signaling.

RESULTS

Schwannomin interacts with HRS

We used the yeast two-hybrid system (21) to identify proteins that interact with schwannomin. Upon screening an adult human brain cDNA library with full-length schwannomin isoform 2 (containing exon 16), a plasmid was identified with a cDNA insert of 2665 bp that encoded the full-length HRS protein of 690 amino acids, determined by automated sequencing (ABI 377 sequencer). This cDNA also included 4 bp of the 5′ UTR sequence and 558 bp of the 3′ UTR sequence preceding the poly(A) sequence.

To demonstrate that the full-length proteins interact *in vivo*, we co-immunoprecipitated HRS from STS26T Schwann cells using an antibody raised against an N-terminal peptide region of schwannomin (ab5991). Detection of immunoprecipitated schwannomin was accomplished with ab5990, raised against a C-terminal peptide region of the protein. Both ab5990 and ab5991 have been well characterized (6,14,15). When immunoprecipitates of ab5991 were analyzed by immunoblotting with ab5990, a single band was observed that was of the same size as schwannomin detected in STS26T cell extracts and schwannomin immunoprecipitated with an anti-HRS antibody, ab1080-2 (Fig. 1A). Likewise, in a reciprocal experiment HRS was co-immunoprecipitated with anti-schwannomin antibody ab5991 (Fig. 1B). We verified the specificity of antibody ab1080-2 by demonstrating that it specifically detected HRS or a green fluorescent protein (GFP)–HRS fusion protein on immunoblots (Fig. 1C and D).

We showed that the interaction between schwannomin and HRS is direct and does not require other cellular factors using an *in vitro* binding assay. A C-terminal schwannomin fragment (residues 299–595) labeled with [^{35}S]methionine interacted specifically with bacterially purified GST–HRS while no significant interaction was observed between schwannomin and GST alone (Fig. 2).

The form of HRS identified in our two-hybrid screen with schwannomin differed from the published human HRS sequence (21,22) by the absence of residues 518–604, encoded by an alternatively spliced exon (Fig. 3). We used primers that anneal upstream (1416A, 5′-AGGACAAGCTGGCACA-GATC-3′) and downstream (2515B, 5′-CAGAGAAGCT-GGAGACCTGAAG-3′) of the apparent splice site and showed that two bands of the predicted sizes (1100 and 1361 bp) representing the two isoforms were amplified from a human brain cDNA library, demonstrating the occurrence of two HRS isoforms in human brain (not shown). To further

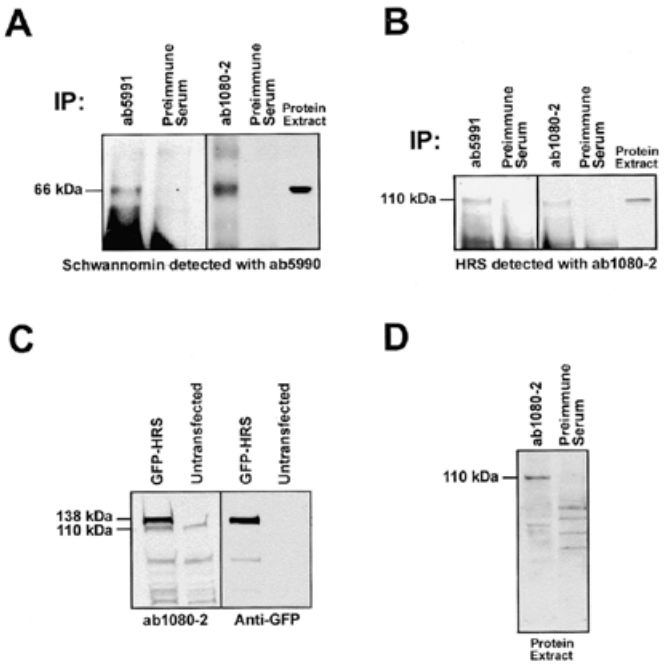

Figure 1. Schwannomin interacts with HRS by co-immunoprecipitation. (**A**) (Left) A schwannomin peptide antibody that recognizes an N-terminal domain epitope (ab5991) immunoprecipitated a schwannomin band of 66 kDa that was absent in immunoprecipitates produced with rabbit preimmune serum. Electrophoresis was conducted on a 6 cm, 4–20% linear gradient polyacrylamide gel. (Right) The HRS antibody, ab1080-2, immunoprecipitated a schwannomin band of the same size as that seen in STS26T cell proteins extracts that was not immunoprecipitated when rabbit preimmune serum was used. Electrophoresis was conducted overnight on a 15 cm, 7.5% SDS–polyacrylamide gel. Both blots were detected with anti-schwannomin antibody ab5990, which recognizes a C-terminal epitope found in both SCHi1 and SCHi2. (**B**) (Left) The schwannomin antibody, ab5991, immunoprecipitated an HRS band of 110 kDa that was absent in immunoprecipitates produced with rabbit preimmune serum. (Right) Anti-HRS antibody ab1080-2 immunoprecipitated an HRS band of the same size as that seen in STS26T cell proteins extracts that was not immunoprecipitated when rabbit preimmune serum was used. Electrophoresis was conducted on a 6 cm, 4–20% linear gradient SDS–polyacrylamide gel and the blots were detected with anti-HRS antibody ab1080-2. (**C**) The anti-HRS antibody ab1080-2 specifically detected a single GFP–HRSi2 band of 138 kDa as well as endogenous HRS of 110 kDa from STS26T cell extracts, while only GFP–HRSi2 was detected with an anti-GFP antibody. (**D**) The specific 110 kDa band visualized by ab1080-2 is not seen when STS26T proteins were detected with the rabbit preimmune serum of the antibody.

support the occurrence of two HRS isoforms, we queried the TIGR database and obtained two plasmids containing parts of the *HRS* gene. Using these plasmids, we verified that both isoforms exist as cloned cDNAs by direct sequencing (GenBank accession nos. N20338 and W56167). We refer to the longer cDNA as *HRS* isoform 1 (encoding HRSi1) and the shorter one identified in our screen as *HRS* isoform 2 (encoding HRSi2).

Schwannomin and HRS interact via their C-terminal halves

HRSi1 interacted more strongly with schwannomin than did HRSi2, as measured in a semi-quantitative liquid assay for β-galactosidase (Fig. 4A; 23). Schwannomin isoform 2 (SCHi2)

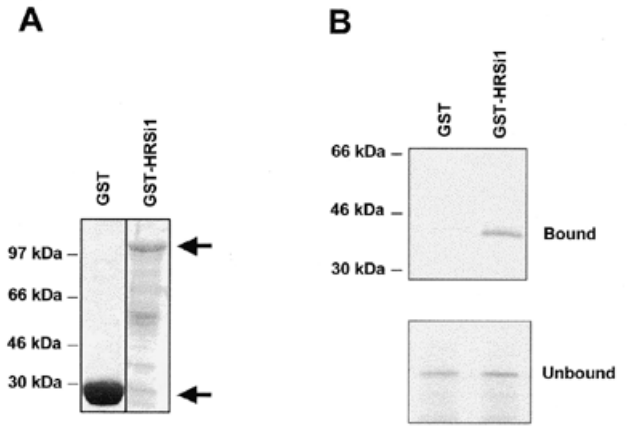

Figure 2. Schwannomin and HRS directly interact. (**A**) Coomassie stained 10% SDS–PAGE gel demonstrating purified GST and the GST–HRSi1 fusion protein. The top arrow denotes GST–HRSi1 (112 kDa) while the bottom arrow denotes GST (26 kDa). (**B**) Affinity chromatography experiments were performed with GST and GST–HRSi1. Binding was observed between the schwannomin C-terminal fragment containing residues 299–595 and GST–HRSi1, but not GST alone. In these experiments both bound and unbound material is shown.

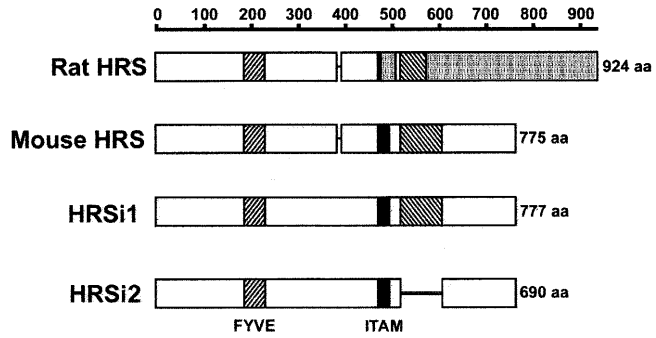

Figure 3. Comparison of human HRS isoforms 1 and 2 with rat and mouse HRS proteins. Each of the rat, mouse and human forms of HRS contains a conserved FYVE ring finger motif (forward hatch fill) and a coiled-coil or ITAM motif (black fill). The portion of the protein that is alternatively spliced in human HRS is indicated (reverse hatch fill). All regions above and below a diagrammed protein are homologous, except for the gray stippled region in rat HRS that is unique to rat. The region between the FYVE and ITAM domains is proline rich and the region downstream of the ITAM domain is proline/glutamine rich. The diagram is modified from Asao *et al.* (20), who also provided estimates of homologies among the species and conducted rigorous coiled-coil predictions. Not shown are putative nucleotide-binding sites, three in human and mouse and four in rat (27).

interacted approximately 10 times more strongly with both HRS isoforms than did schwannomin isoform 1 (SCHi1, lacking exon 16). To map the HRS-binding domain in schwannomin, we generated N- and C-terminally deleted fragments of schwannomin. A schwannomin deletion protein terminating in the middle of exon 15 retained strong HRS binding, as did schwannomins deleted of the N-terminal half (Fig. 4A). A truncated schwannomin with only the N-terminal domain (residues 1–304) did not bind HRS (Fig. 4A). Therefore, the HRS-binding region is in the schwannomin C-terminal half, between schwannomin residues 256 and 579, consistent with the GST interaction results (Fig. 2). In addition, HRSi1 bound to a C-terminal schwannomin fragment of residues 256–590 more strongly than did HRSi2, and HRSi2 bound to C-terminal schwannomin fragments of residues 363–590, 422–590 and 469–590 more strongly than did HRSi1. This suggests that schwannomin residues 256–363 strengthen the interaction with HRSi1 but not with HRSi2 and that HRSi2 may have a smaller schwannomin-binding region. In addition, all C-terminal truncated SCHi2 fragments interacted more weakly than did full-length SCHi2, suggesting that the N-terminal domain may strengthen these interactions.

We also tested the ability of schwannomin to interact with HRS deletions by the yeast two-hybrid method. Schwannomin did not interact with a HRS partial protein of residues 1–480, but schwannomin strongly interacted with a HRSi2 partial protein of residues 327–690 (Fig. 4B). These data demonstrate that schwannomin binds the C-terminal half of both HRS isoforms downstream of residue 480.

Mutant schwannomins have altered binding to HRS

A number of *NF2* missense mutations are associated with milder patient phenotypes. Phenotype severity may be the result of altered interaction between schwannomin and its binding proteins. To assess the effect of *NF2* missense mutation on HRS binding, we used the yeast two-hybrid system to evaluate changes in binding strengths between HRSi1 and HRSi2 and SCHi2 containing naturally occurring missense mutations. We previously demonstrated high expression of these mutant schwannomins in yeast (14). Each of the tested *NF2* missense mutations significantly reduced HRS binding, but did not completely abolish HRS interaction. Only the interaction between schwannomin L360P and HRSi2 was similar to the control, indicating an almost complete loss of binding. On the other hand, amino acid substitution in the schwannomin N-terminal domain (L46R) affected binding much less than C-terminal domain substitutions.

Schwannomin and HRS co-localize

We employed confocal microscopy to demonstrate co-localization of HRS and schwannomin by two methods: (i) co-localization of schwannomin with exogenous HRS; (ii) co-localization of endogenous HRS and endogenous schwannomin. We overexpressed Xpress epitope tagged (xp) HRSi1 in STS26T cells and co-labeled with anti-Xpress antibody and the schwannomin antibody ab5990. Confocal microscopy showed complete co-localization of xp-HRSi1 and endogenous schwannomin to cytoplasmic regions (Fig. 5A). Additionally, schwannomin was redistributed in transfected cells expressing xp-HRSi1, which had fewer, larger punctata than did untransfected cells (Fig. 5A). We also co-labeled endogenous HRS and schwannomin with HRS-specific polyclonal antibody ab1080-2 and an NF2 monoclonal antibody to reveal co-localization in perinuclear and cytoplasmic structures (Fig. 5B).

To explore the possibility that the co-localization of HRS and schwannomin occurred in endosomes, we co-labeled STS26T cells with an antibody raised against early endosome antigen 1 (EEA1) and either the HRS antibody ab1080-2 or schwannomin antibody ab5990. EEA1 co-localizes with Rab5 in early endosomes and, as for HRS, endosomal localization of

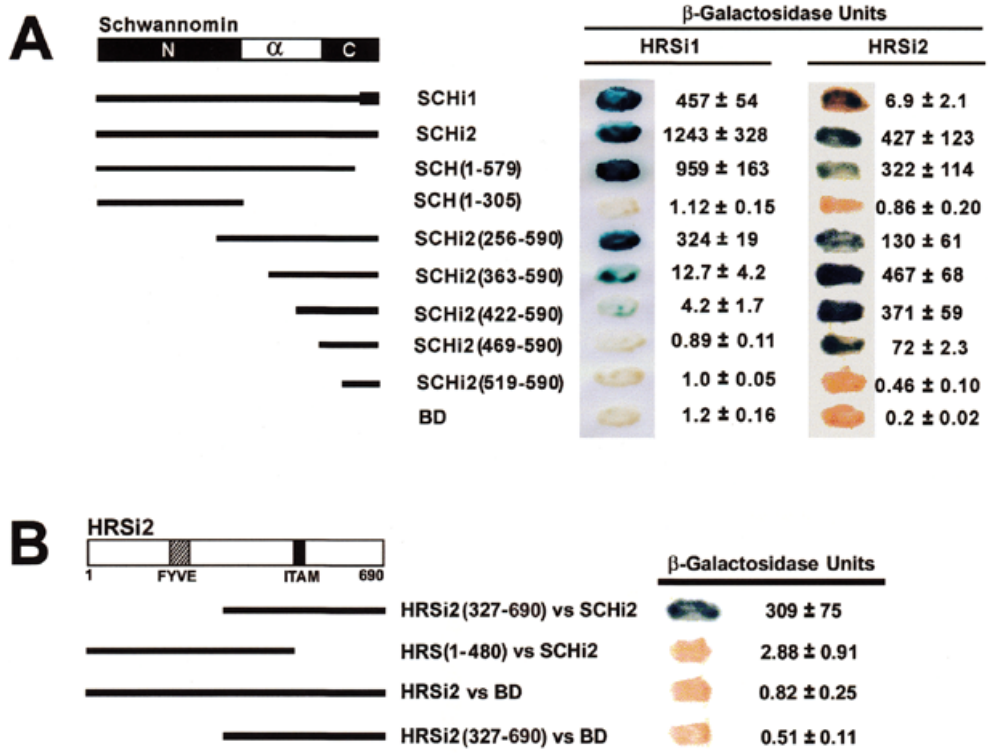

Figure 4. Yeast two-hybrid tests of interaction narrowed the interacting regions in HRS and schwannomin. (**A**) Tests of interaction between HRS isoforms, encoded by pGAD10, and the indicated schwannomin proteins encoded by pGBT9 demonstrated that HRS binds the C-terminal half of schwannomin, between schwannomin residues 256 and 579. Because HRSi1 bound to SCHi2 residues 256–590 more strongly than did HRSi2 and HRSi2 bound to SCHi2 residues 363–590, 422–590 and 469–590 more strongly than did HRSi1, schwannomin residues 256–363 strengthen the interaction with HRSi1 but not with HRSi2. Tests conducted with SCHi1 demonstrated a weaker interaction than for full-length SCHi2. However, tests with SCHi1 partial proteins possessing the C-terminal region interacted strongly, suggesting that both schwannomin isoforms may have a significant functional role involving HRS (not shown). The drawing illustrates schwannomin and its three major domains, N-terminal, α-helical and C-terminal. (**B**) Tests of interaction conducted between HRS or HRS partial proteins encoded by pGAD10-HRSi2 and full-length SCHi2 encoded by pGBT9-NF2i2 demonstrated that schwannomin binds the C-terminal half of HRS. The diagram depicts the locations of the FYVE and ITAM domains of the HRS protein. Blue indicates the presence of β-galactosidase and a positive test of interaction between encoded proteins. In control tests BD denotes the GAL4-binding domain encoded by pGBT9 with no insert.

EEA1 is mediated by a FYVE domain (24). We observed that all of the EEA1 labeling co-localized with HRS or schwannomin in cytoplasmic punctata (Fig. 5C and D).

DISCUSSION

The NF2 tumor suppressor is one of the most commonly altered proteins in human CNS tumors. Virtually all Schwann cell tumors bear *NF2* mutations or deletions and *NF2* gene alterations are also common in meningiomas and ependymomas. Despite this, the precise role of schwannomin as a tumor suppressor has remained undefined. The considerable homology of the N-terminal half of schwannomin with the ERM family of proteins provided clues as to its subcellular location, but has not provided insight into schwannomin function, since signaling pathways mediated by this domain in ERM proteins are not known. Previous studies showed that schwannomin interacts with NHERF/EBP50 and βII-spectrin, consistent with a location at the cell membrane and the cytoskeleton, but did not implicate schwannomin in any specific signal transduction pathway (14,25,26). The search for a target of schwannomin action was further complicated by the fact that little is known about Schwann cell mitogens and the downstream signals induced by these growth factors.

The mammalian form of HRS was initially identified as a protein of 777 amino acids that was phosphorylated upon HGF stimulation (22). Our yeast two-hybrid screen identified an isoform of HRS that had not been previously isolated (designated HRSi2). The HRSi2 cDNA sequence isolated from adult brain predicts a protein of 690 amino acids in length. This sequence differed in part from the previous human (20) and mouse HRS (22) sequences in that DNA encoding amino acids 518–604 was absent due to alternative splicing. The form of HRS identified in rat has never been observed in humans and differs considerably in the C-terminal half of the protein (Fig. 2; 27). Both human HRS isoforms bound schwannomin, although the binding of HRSi1 was stronger (Table 1). Binding between schwannomin and HRS is strong and occurs at physiological concentrations, since both endogenous proteins were co-immunoprecipitated from STS26T cells using either anti-schwannomin or anti-HRS antibody (Fig. 1). We narrowed the regions of interaction to residues 256–579 of both schwannomin isoforms and from residue 480 to the end of the two HRS isoforms and we showed that schwannomin residues 256–363 enhance HRSi1 binding but not HRSi2 binding.

The interactions between schwannomin and HRS may be modified by the conformations of the molecules. The interaction with HRS was stronger with full-length schwannomin

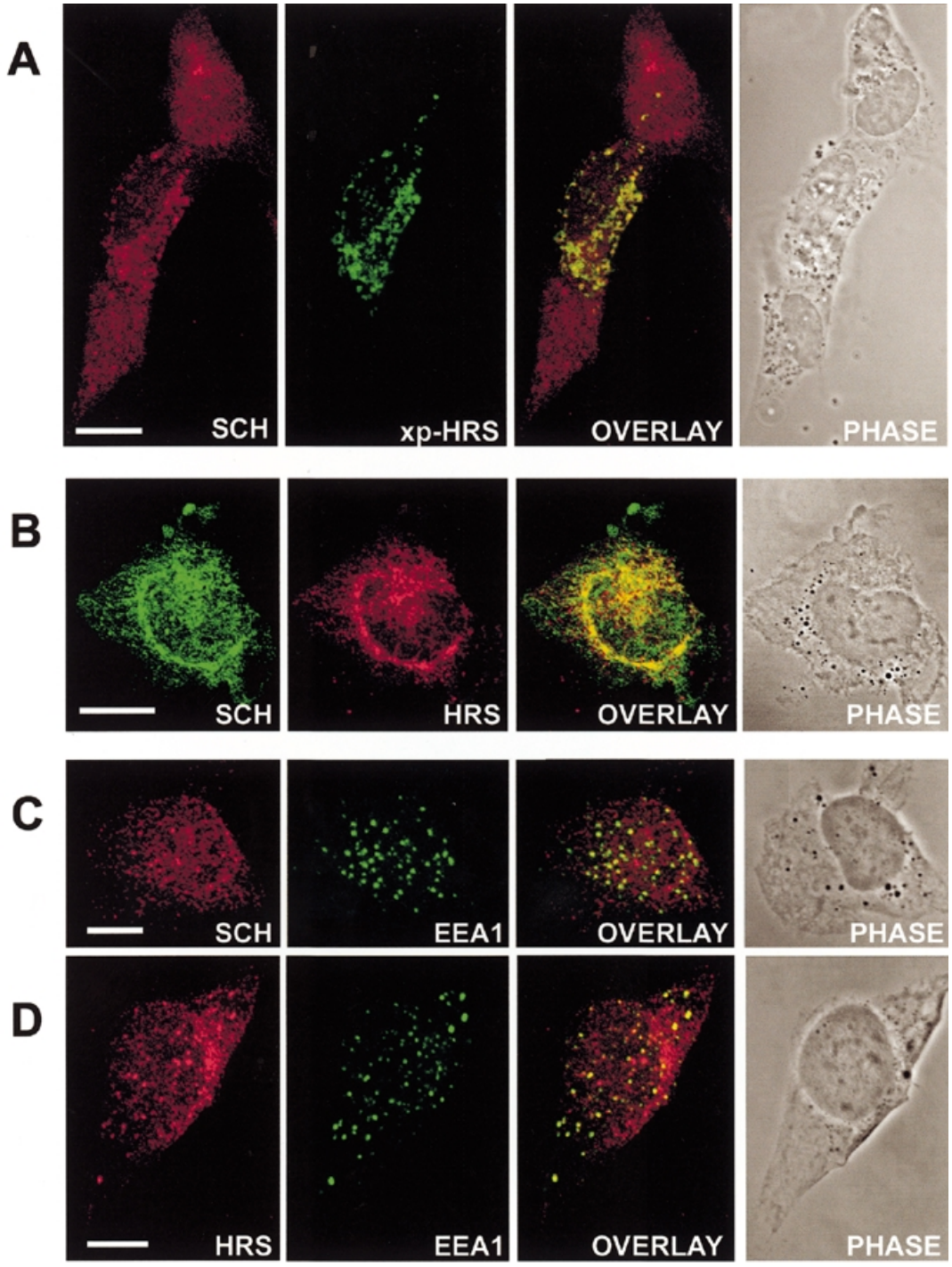

Figure 5. Schwannomin and HRS co-localize in STS26T cells. (**A**) STS26T cells transfected to express Xpress tagged (xp) HRSi1 and co-labeled with anti-Xpress monoclonal antibody and the anti-schwannomin antibody ab5990 revealed near total co-localization of both proteins. Note that the transfected cell (the center cell of the three shown) showed schwannomin reorganization to fewer, larger punctata. (**B**) Labeling of endogenous schwannomin with an anti-schwannomin monoclonal antibody and endogenous HRS with ab1080-2 revealed strong co-localization in perinuclear regions and also in cytoplasmic structures. (**C**) Immunofluorescent co-labeling with ab5990 and anti-EEA1 antibody demonstrated partial localization of schwannomin on early endosomes. All EEA1 labeling co-localized with schwannomin labeling. (**D**) Immunofluorescent co-labeling with ab1080-2 and anti-EEA1 antibody demonstrated partial localization of HRS on early endosomes. All EEA1 labeling co-localized with HRS labeling.

than with any of the truncated schwannomins (Fig. 4). This suggests that other regions of schwannomin, outside the minimally interacting regions identified in our study, may stabilize this interaction. In addition, HRSi1 bound SCHi2 more than 2.5 times more strongly than SCHi1 and HRSi2 bound SCHi2 more than 60 times more strongly than SCHi1 (Fig. 4). Previous work by one of us (D.H.G.) has demonstrated that schwannomin function is dictated by its ability to form produc-

Table 1. Binding of mutant schwannomins with HRS

	pGAD10-HRSi1	PGAD10-HRSi2
pGBT9	2.3 ± 0.5	1.2 ± 0.3
pGBT9-NF2i2	1252 ± 98	319 ± 82
pGBT9-NF2i2(L46R) (39)	391 ± 102	25.4 ± 3.0
pGBT9-NF2i2(L360P) (40)	66.8 ± 35.0	1.7 ± 0.6
pGBT9-NF2i2(L535P) (41)	47.6 ± 7.2	11.1 ± 2.4
pGBT9-NF2i2(Q538P) (37)	50.0 ± 11.0	8.5 ± 1.1

pGBT9 constructs encoding SCHi2 (NF2i2) or SCHi2 molecules containing the L46R, L360P, L535P or Q538P missense mutation were co-transformed with pGAD10-HRSi1 or HRSi2 encoding full-length HRS. β-Galactosidase activity ± SD is shown for each interaction. Experiments were conducted in triplicate.

tive intramolecular associations (28). Schwannomin containing exon 16 (SCHi2) cannot form a productive intramolecular association, in contrast to SCHi1 lacking exon 16 (29). In this fashion, schwannomin intramolecular interactions, regulated by the alternative splicing of exon 16, may regulate binding to HRS. We expect that loss of these interactions by *NF2* truncating or missense mutation alters pathways modulated by HRS.

The subcellular distribution of HRS in STS26T cells (Fig. 5A–C) is consistent with previous observations of its localization at the cytoplasmic surface of early endosomes (30). Schwannomin co-localized with HRS on early endosomes in STS26T cells at punctate structures (Fig. 5A–D). In view of the fact that much of the schwannomin labeling in mammalian cells is reported at the cell membrane (9), it was puzzling that the *Drosophila* schwannomin ortholog localized to endocytic vesicles (31). We and others had previously observed punctate labeling for schwannomin in addition to labeling at the cell membrane (14,12) and now show that most of these schwannomin punctata in STS26T cells are also positive for the early endosome marker EEA1 (Fig. 5C).

HRS may be implicated in two distinct functions. HRS is a ubiquitous FYVE zinc ring finger protein that is tyrosine phosphorylated in response to the cytokines platelet-derived growth factor (PDGF), HGF, epidermal growth factor, interleukin-2 and interleukin-3/granulocyte-macrophage colony stimulating factor (GM-CSF) (20,22). HRS binds phosphatidylinositol (3)-phosphate and is localized on endosomes (29,32,33). In *Saccharomyces cerevisiae* deficiency in Vps27p, the highly conserved HRS ortholog, results in accumulation of membrane proteins and receptors on endosomes, resulting in their recycling to the plasma membrane instead of sorting to the vacuole lumen (18). Co-localization of schwannomin with HRS on early endosomes suggests a possible role for schwannomin in sorting of membrane receptors.

A second proposed function for HRS is in JAK/STAT signaling. HRS interacts with the signal transduction adapter molecule STAM, which is a ubiquitous protein involved in cytokine-mediated signal transduction. STAM in turn binds JAK2 and JAK3, which are essential for STAT-mediated induction of c-*myc*, c-*fos* and DNA synthesis upon growth factor stimulation in BAF-B03 cells (19,34,35). HRS can suppress these signals in BAF-B03 cells, but not when HRS is deleted for the STAM-binding site (20). We have preliminary data that show that overexpression of schwannomin suppresses STAT signaling in a manner requiring HRS interaction (Scoles *et al*., in preparation). It is not known whether the endosomal localization of schwannomin and HRS is connected to HRS interaction with STAM and down-regulation of STAT activation or represents an independent function of schwannomin/HRS on endosomes. The identification of HRS as a schwannomin binder may lead to novel approaches to Schwann cell biology with regard to receptor endocytosis and STAT signaling.

MATERIALS AND METHODS

Accession number

The GenBank accession no. for the HRSi2 sequence reported in this paper is AF260566.

Identification of schwannomin interacting proteins

A yeast two-hybrid screen (21) of a human adult brain cDNA library cloned in GAL4 activation domain vector pGAD10 was accomplished using pGBT9NF2i2, encoding SCHi2 fused to the GAL4-binding domain (see ref. 14) (vectors and library from Clontech, Palo Alto, CA). A plasmid containing the complete HRS cDNA was purified and retransformed with pGBT9NF2i2, pGBT9NF2i1, encoding SCHi1, or pGBT9NF2i2 partial deletions or mutants. Yeast strain Y190 double transformants were grown on SC medium with leucine, tryptophan and histidine removed and with 25 mM 3-amino-1,2,4-triazole and 2% glucose (23). β-Galactosidase production was assayed by incubating freeze-fractured colonies on nitrocellulose in Z buffer (60 mM Na_2HPO_4, 40 mM NaH_2PO_4, 10 mM KCl, 1 mM $MgSO_4$, pH 7.0, 0.03 mM β-mercaptoethanol and 2.5 μM X-gal) at 37°C for 15–480 min. Liquid assays for β-galactosidase were conducted by incubating yeast extracted in Z buffer and 5% chloroform with 0.6 mg/ml *o*-nitrophenylgalactoside for 2–60 min. β-Galactosidase units = $1000 \times [OD_{420}/(OD_{600} \times \text{time} \times \text{volume})]$ (23).

Plasmid constructs

Cloning of HRSi1. HRSi2 was modified to encode HRSi1. The pGAD10-HRSi2 plasmid was digested with *Bsa*I, which cuts in the *HRS* gene 3′ UTR and in the β-lactamase gene of pGAD10, and with *Sma*I, which cuts at position 1439 of the *HRS* gene. pGAD10-HRSi1 was directionally cloned by ligating the two fragments retaining both halves of the β-lactamase gene in a three-way fashion to the HRSi1 C-terminal half excised from a plasmid identified by screening the TIGR database (GenBank accession no. N20338) by *Sma*I and *Bsa*I digestion. Only properly orientated ligation products restored β-lactamase function and were ampicillin resistant.

To prepare an expression construct of HRS, full-length HRSi1 was excised from pGAD10-HRSi1 with *Sal*I and ligated at the *Sal*I site of pcDNA3.1his (Invitrogen, Carlsbad, CA). For expression of HRS as a GFP fusion, the full-length HRSi2 was excised from pGAD10-HRSi2 with *Sal*I and ligated at the *Sal*I site of pEGFPC (Clontech).

Methods for the construction of pGBT9 plasmids encoding schwannomins with missense mutations were described previously (14).

Antibodies

Rabbit polyclonal antibody ab5990 was raised against schwannomin residues 527–541 (EYMEKSKHLQEQLNE) and ab5991 was raised against schwannomin residues 10–22 (SFSSLKRKQPKTF) as previously described (2,15). Rabbit polyclonal antibody ab1080-2 was raised against HRS residues 119–132 (FRNEPKYKVVQDTY) using previously described methods (15). GFP fusion proteins were detected using rabbit polyclonal anti-GFP (Clontech). The Xpress epitope tag encoded on pcDNA3.1his was detected with anti-Xpress antibody (Invitrogen). Monoclonal antibodies were used to detect schwannomin and EEA1 (Transduction Laboratories, Lexington, KY). Antibodies ab5990, ab5991 and ab1080-2 were affinity purified for immunoblotting, immunohistochemical staining or immunofluorescent staining as previously described (36) or antisera were used directly for immunoprecipitation.

Immunoprecipitation

STS26T cells were used for functional analyses because they are a relevant cell type that are of Schwann cell origin (S100-positive; ref. 15) that originate from a malignant grade III schwannoma (37). STS26T cells were grown in Dulbecco's modified Eagle's medium (DMEM) with 10% fetal bovine serum in the presence of penicillin and streptomycin. Cells were homogenized in buffer A [20 mM Tris, pH 8.0, 150 mM NaCl, 0.1% Igepal CA-630 (Sigma, St Louis, MO), 0.5% deoxycholic acid, 2 µg/ml aprotinin, 1 µg/ml leupeptin, 1 µg/ml pepstatin A and 0.5 mg/ml Pefabloc SC]. Formalin-fixed *Staphylococcus aureus* cells (Sigma) were added to 4% and the mixture was incubated for 30 min at 4°C. The *S.aureus* cells were removed by centrifugation and this step was repeated. For each immunoprecipitation, 10 µg of cleared lysate protein was mixed with 0.5–2 µl of antiserum or preimmune serum in a volume of 1 ml of buffer A and rotated for 1 h at room temperature. Thereafter, 50 µl of a 50% slurry of protein A/G–Sepharose (CytoSignal Research Products, Irvine, CA) was added and the mixtures were rotated for 1 h. Protein complexes binding the protein A–Sepharose were collected by centrifugation for 15 s and washed four times in buffer A. The mixture was transferred to a spin column (CytoSignal Research Products) and proteins were eluted over 15 min in 50 µl of 1× Laemmli buffer. Aliquots of 14 µl were used for SDS–PAGE and immunoblotting. Samples were heat denatured before gel analysis.

In vitro binding assay

GST fusion proteins were prepared for the interaction experiments with *in vitro* transcribed and translated schwannomin proteins as previously described (38,39). Briefly, full-length HRSi1 was generated by PCR (Gutmann *et al.*, manuscript in preparation) and sequenced prior to cloning into pGEX.3X (Pharmacia, Piscataway, NJ). pGEX.3X and pGEX.3X.HRSi1 were transformed into DE3 (BL21) competent cells, induced overnight with 0.4 mM IPTG at room temperature and fusion proteins collected on glutathione–agarose beads (Sigma).

In vitro transcribed and translated C-terminal schwannomin (residues 299–595) protein was synthesized in the presence of [^{35}S]methionine using the TnT protocol (Promega, Madison, WI) according to the instructions supplied by the manufacturer. Radiolabeled C-terminal schwannomin was then incubated with equimolar amounts of GST and GST–HRSi1 fusion proteins immobilized on glutathione–agarose beads for 2 h at 4°C. The unbound fraction was saved and the agarose beads were then washed four times in TEN buffer (10 mM Tris, pH 7.5, 150 mM NaCl, 5 mM EDTA and 1% Triton X-100) and eluted in 1× Laemmli buffer. An equal fraction of the supernatant and eluted bound fraction was separated by SDS–PAGE and analyzed by autoradiography. In all experiments no significant binding was observed with immobilized GST (<2% total bound).

Immunofluorescence

STS26T cells (30 000 cells/well in 4-well slides) were grown in DMEM with 10% fetal bovine serum overnight. Cells were labeled for immunofluorescence as previously described (14,15). The primary antibody dilutions were 5 µg/ml ab5990, 20 µg/ml ab1080-2, 4 µg/ml anti-STAT3, 1:100 anti-schwannomin mAb, 1:500 anti-EEA1 mAb and 1:500 anti-Xpress mAb. Primary antibodies were incubated for 60 min at 37°C. Following three washes with cold Dulbecco's phosphate-buffered saline (DPBS), cells were incubated with rhodamine-conjugated affinity-purified goat anti-rabbit IgG (Sigma) or FITC-conjugated affinity-purified goat anti-mouse IgG (Sigma) for 1 h at room temperature, washed six times in cold DPBS and mounted. Fluorescence confocal microscopy was performed using a Zeiss LSM 310 confocal microscope (Carl Zeiss, Thornwook, NY). FITC or GFP were visualized with a BP485/20/BP520-560 excitation/emission filter set (Zeiss filter set 17) and scanning was with a 488 nm argon laser and a BP520-560 barrier filter. Rhodamine visualization was with a BP515-560/LP590 excitation/emission filter set (Zeiss filter set 15) and scanning was with a 543 nm HeNe laser and an LP590 nm barrier filter.

ACKNOWLEDGEMENTS

We thank Matt Schibler for assistance with the confocal microscopy, Diane H.D. Ho for assistance with the co-immunoprecipitation and Carrie A. Haipek for assistance with the *in vitro* interaction studies. This work was supported by the Steven and Lottie Walker Foundation and the Carmen and Louis Warschaw Endowment Fund. Support was also provided by grants NS01428-01A1 from the National Institutes of Health (NIH) and DAMD17-99-1-9548 from the Department of Defense to S.M.P., NS35848 from the NIH to D.H.G. and NIH National Research Service Award NS10524-02 to D.R.S.

REFERENCES

1. Mautner, V.F., Lindenau, M., Baser, M.E., Hazim, W., Tatagiba, M., Haase, W., Samii, M., Wais, R. and Pulst, S.M. (1996) The neuroimaging and clinical spectrum of neurofibromatosis 2. *Neurosurgery*, **38**, 880–885.
2. Sainz, J., Huynh, D.P., Figueroa, K., Ragge, N.K., Baser, M.E. and Pulst, S.M. (1994) Mutations of the neurofibromatosis type 2 gene and lack of

the gene product in vestibular schwannomas. *Hum. Mol. Genet.*, **3**, 885–891.
3. Ruttledge, M.H., Sarrazin, J., Rangaratnam, S., Phelan, C.M., Twist, E., Merel, P., Delattre, O., Thomas, G., Nordenskjöld, M. *et al.* (1994) Evidence for the complete inactivation of the NF2 gene in the majority of sporadic meningiomas. *Nature Genet.*, **6**, 180–184.
4. Rubio, M.P., Correa, K.M., Ramesh, V., MacCollin, M.M., Jacoby, L.B., von Deimling, A., Gusella, J.F. and Louis, D.N. (1994) Analysis of the Neurofibromatosis 2 gene in human ependymomas and astrocytomas. *Cancer Res.*, **54**, 45–47.
5. Gutmann, D.H., Giordano, M.J., Fishback, A.S. and Guha, A. (1997) Loss of merlin expression in sporadic meningiomas, ependymomas and schwannomas. *Neurology*, **49**, 267–270.
6. Huynh, D.P., Mautner, V., Baser, M.E., Stavrou, D. and Pulst, S.M. (1997) Immunohistochemical detection of schwannomin and neurofibromin in vestibular schwannomas, ependymomas and meningiomas. *J. Neuropathol. Exp. Neurol.*, **56**, 382–390.
7. Rouleau, G.A., Merel, P., Lutchman, M., Sanson, M., Zucman, J., Marineau, C., Xuan, K.H., Demczuk, S., Desmaze, C., Plougastel, B. *et al.* (1993) Alteration in a new gene coding a putative membrane-organizing protein causes neuro-fibromatosis type 2. *Nature*, **363**, 515–521.
8. Trofatter, J.A., MacCollin, M.M., Rutter, J.L., Murrell, J.R., Duyao, M.P., Parry, D.M., Eldridge, R., Kley, N., Menon, A., Pulaski, K. *et al.* (1993) A novel moesin-, ezrin-, radixin-like gene is a candidate for the neurofibromatosis 2 tumor suppressor. *Cell*, **72**, 791–800.
9. Gonzalez-Agosti, C., Xu, L., Pinney, D., Beauchamp, R., Hobbs, W., Gusella, J. and Ramesh, V. (1996) The merlin tumor suppressor localizes preferentially in membrane ruffles. *Oncogene*, **13**, 1239–1247.
10. Scherer, S.S. and Gutmann, D.H. (1996) Expression of the neurofibromatosis 2 tumor suppressor gene product, merlin, in Schwann cells. *J. Neurosci. Res.*, **46**, 595–605.
11. Pelton, P.D., Sherman, L.S., Rizvi, T.A., Marchionni, M.A., Wood, P., Friedman, R.A. and Ratner, N. (1998) Ruffling membrane, stress fiber, cell spreading and proliferation abnormalities in human Schwannoma cells. *Oncogene*, **17**, 195–209.
12. Xu, L., Gonzalez-Agosti, C., Beauchamp, R., Pinney, D., Sterner, C. and Ramesh, V. (1998) Analysis of molecular domains of epitope-tagged merlin isoforms in Cos-7 cells and primary rat Schwann cells. *Exp. Cell Res.*, **238**, 231–240.
13. Xu, H.M. and Gutmann, D.H. (1998) Merlin differentially associates with the microtubule and actin cytoskeleton. *J. Neurosci. Res.*, **51**, 403–415.
14. Scoles, D.R., Huynh, D.P., Morcos, P.A., Coulsell, E.R., Robinson, N.G.G., Tamanoi, F. and Pulst, S.M. (1998) Neurofibromatosis 2 tumor suppressor schwannomin interacts with βII-spectrin. *Nature Genet.*, **18**, 354–359.
15. Huynh, D.P. and Pulst, S.M. (1996) Neurofibromatosis 2 antisense oligodeoxynucleotides induce reversible inhibition of schwannomin synthesis and cell adhesion in STS26T and T98G cells. *Oncogene*, **13**, 73–84.
16. Gutmann, D.H., Sherman, L., Seftor, L., Haipek, C., Hoang Lu, K. and Hendrix, M. (1999) Increased expression of the NF2 tumor suppressor gene product, merlin, impairs cell motility, adhesion and spreading. *Hum. Mol. Genet.*, **8**, 267–75.
17. Krasnoselsky, A., Massay, M.J., DeFrances, M.C., Michalopoulos, G., Zarnegar, R. and Ratner, N. (1994) Hepatocyte growth factor is a mitogen for Schwann cells and is present in neurofibromas. *J. Neurosci.*, **14**, 7284–7290.
18. Odorizzi, G., Babst, M. and Emr, S.D. (1998) Fab1p PtdIns (3)P 5-kinase function essential for protein sorting in the multivesicular body. *Cell*, **95**, 847–858.
19. Takeshita, T., Arita, T., Higuchi, M., Asao, H., Endo, K., Kuroda, H., Tanaka, N., Murata, K., Ishii, N. and Sugamura, K. (1997) STAM, signal transducing adaptor molecule, is associated with Janus kinases and involved in signaling for cell growth and c-myc induction. *Immunity*, **6**, 449–457.
20. Asao, H., Sasaki, Y., Arita, T., Tanaka, N., Endo, K., Kasai, H., Takeshita, T., Endo, Y., Fujita, T. and Sugamura, K. (1997) Hrs is associated with STAM, a signal-transducing adaptor molecule: its suppressive effect on cytokine-induced cell growth. *J. Biol. Chem.*, **272**, 32785–32791.
21. Fields, S. and Song, O.-k. (1989) A novel genetic system to detect protein-protein interactions. *Nature*, **340**, 245–246.
22. Komada, M. and Kitamura, N. (1995) Growth factor-induced tyrosine phosphorylation of HRS, a novel 115-kilodalton protein with a structurally conserved putative zinc finger domain. *Mol. Cell. Biol.*, **15**, 6213–6221.
23. Poullet, P. and Tamanoi, T. (1995) Use of the yeast two-hybrid system to evaluate ras interactions with neurofibromin GTP-ase activating proteins. *Methods Enzymol.*, **255**, 488–497.
24. Stenmark, H., Aasland, R., Toh, B.H. and D'Arrigo, A. (1996) Endosomal localization of the autoantigen EEA1 is mediated by a zinc-binding FYVE finger. *J. Biol. Chem.*, **271**, 24048–24054.
25. Reczek, D., Berryman, M. and Bretscher, A. (1997) Identification of EBP50: a PDZ-containing phosphoprotein that associates with members of the ezrin-radixin-moesin family. *J. Cell Biol.*, **139**, 169–179.
26. Murthy, A., Gonzalez-Agosti, C., Cordero, E., Pinney, D., Candia, C., Solomon, F., Gusella, J. and Ramesh, V. (1998) NHE-RF, a regulatory cofactor for Na(+)-H+ exchange, is a common interactor for merlin and ERM (MERM) proteins. *J. Biol. Chem.*, **273**, 1273–1276.
27. Bean, A.J., Seifert, R., Chen, Y.A., Sacks, R. and Scheller, R.H. (1997) HRS-2 is an ATPase implicated in calcium-regulated secretion. *Nature*, **385**, 826–829.
28. Gutmann, D.H., Geist, R.T., Xu, H.-M., Kim, J.S. and Saporito-Irwin, S. (1998) Defects in neurofibromatosis 2 protein function can arise at multiple levels. *Hum. Mol. Genet.*, **7**, 335–345.
29. Gutmann, D.H., Haipek, C.A. and Hoang, L.K. (1999) Neurofibromatosis 2 tumor suppressor protein, merlin, forms two functionally important intramolecular associations. *J. Neurosci. Res.*, **58**, 706–716.
30. Komada, M., Masaki, R., Yamamoto, A. and Kitamura, N. (1997) HRS, a tyrosine kinase substrate with a conserved double zinc finger domain, is localized to the cytoplasmic surface of early endosomes. *J. Biol. Chem.*, **272**, 20538–20544.
31. McCartney, B.M. and Fehon, R.G. (1996) Distinct cellular and subcellular patterns of expression imply distinct functions for the *Drosophila* homologues of moesin and the neurofibromatosis 2 tumor suppressor, merlin. *J. Cell Biol.*, **133**, 843–852.
32. Burd, C.G. and Emr, S.D. (1999) Phosphatidylinositol(3)-phosphate signaling mediated by specific binding to ring FYVE domains. *Mol. Cell*, **2**, 157–162.
33. Gaullier, J.M., Simonsen, A., D'Arrigo, A., Bremnes, B., Stenmark, H. and Aasland, R. (1998) FYVE fingers bind PtdIns(3)P. *Nature*, **394**, 432–433.
34. Kawahara, A. Minami, Y., Miyazaki, T., Ihle, J.N. and Taniguchi, T. (1995) Critical role of the interleukin 2 (IL-2) receptor γ-chain-associated Jak3 in the IL-2-induced c-*fos* and c-*myc*, but not *bcl-2*, gene induction. *Proc. Natl Acad. Sci. USA*, **92**, 8724–8728.
35. Watanabe, S., Itoh, T. and Arai, K. (1996) JAK2 is essential for activation of c-*fos* and c-*myc* promoters and cell proliferation through the human granulocyte-macrophage colony-stimulating factor receptor in BA/F3 cells. *J. Biol. Chem.*, **271**, 12681–12686.
36. Huynh, D.P., Nechiporuk, T. and Pulst, S.M. (1994) Differential expression and tissue distribution of type I and type II neurofibromin during mouse fetal development. *Dev. Biol.*, **161**, 538–551.
37. Dahlberg, W.K., Little, J.B., Fletcher, J.A., Suit, H.D. and Okunieff, P. (1993) Radiosensitivity *in vitro* of human soft tissue carcinoma cell lines and skin fibroblasts derived from the same patients. *Int. J. Radiat. Biol.*, **63**, 191–198.
38. Kluwe, L. and Mautner, V.F. (1996) A missense mutation in the *NF2* gene results in moderate and mild clinical phenotypes of neurofibromatosis type 2. *Hum. Genet.*, **97**, 224–227.
39. Sherman, L., Xu, H.-M., Geist, R.T., Saporito-Irwin, S., Howells, N., Ponta, H., Herrlich, P. and Gutmann, D.H. (1997) Interdomain binding mediates tumor growth suppression by the *NF2* gene product. *Oncogene*, **15**, 2505–2509.
40. Irving, R.M., Moffat, D.A., Hardy, D.G., Barton, D.E., Xuereb, J.H. and Maher, E.R. (1994) Somatic *NF2* gene mutations in familial and non-familal vestibular schwannoma. *Hum. Mol. Genet.*, **3**, 347–350.
41. Merel, P., Hoang-Xuan, K., Sanson, M., Bijlsma, E., Rouleau, G., Laurent-Puig, P., Pulst, S., Baser, M., Lenoir, G., Sterkers, J.M. *et al.* (1995) Screening for germline mutations in the *NF2* gene. *Genes Chromosomes Cancer.*, **12**, 117–127.
42. Evans, D.G.R., Bourn, D., Wallace, A., Ramsden, R.T., Mitchell, J.D. and Strachan, T. (1995) Diagnosis issues in a family with late onset type 2 neurofibromatosis. *J. Med. Genet.*, **32**, 470–474.